Articles

Catalytic Acid−Base Groups in Yeast Pyruvate Decarboxylase. 1. Site-Directed Mutagenesis and Steady-State Kinetic Studies on the Enzyme with the D28A, H114F, H115F, and E477Q Substitutions†

Min Liu,‡ Eduard A. Sergienko,‡ Fusheng Guo,‡ Jue Wang,‡ Kai Tittmann,§ Gerhard Hübner,§ William Furey,⊥ and Frank Jordan*,‡

Department of Chemistry and Program in Cellular and Molecular Biodynamics, Rutgers, The State University of New Jersey, Newark, New Jersey 07102, Department of Biochemistry, Martin-Luther-University, Halle, Germany, and Department of Pharmacology, University of Pittsburgh School of Medicine, Pittsburgh, PA 15261 and the VA Medical Center Biocrystallography Laboratory, Pittsburgh, PA 16240

Received December 18, 2000; Revised Manuscript Received April 17, 2001

ABSTRACT: The roles of four of the active center groups with potential acid−base properties in the region of pH optimum of pyruvate decarboxylase from *Saccharomyces cerevisiae* have been studied with the substitutions Asp28Ala, His114Phe, His115Phe, and Glu477Gln, introduced by site-directed mutagenesis methods. The steady-state kinetic constants were determined in the pH range of activity for the enzyme. The substitutions result in large changes in k_{cat} and $k_{cat}/S_{0.5}$ (and related terms), indicating that all four groups have a role in transition state stabilization. Furthermore, these results also imply that all four are involved in some manner in stabilizing the rate-limiting transition state(s) both at low substrate (steps starting with substrate binding and culminating in decarboxylation) and at high substrate concentration (steps beginning with decarboxylation and culminating in product release). With the exception of some modest effects, the shapes of neither the bell-shaped $k_{cat}/S_{0.5}$−pH (and related functions) plots nor the k_{cat}−pH plots are changed by the substitutions. Yet, the fractional activity still remaining after substitutions virtually rules out any of the four residues as being directly responsible for initiating the catalytic process by ionizing the C2H. There is no effect on the C2 H/D exchange rate exhibited by the D28A and E477Q substitutions. These results strongly imply that the base-induced deprotonation at C2 is carried out by the only remaining base, the iminopyrimidine tautomer of the coenzyme, via intramolecular proton abstraction. The first product is released as CO_2 rather than HCO_3^- by both wild-type and E477Q and D28A variants, ruling out several mechanistic alternatives.

Yeast pyruvate decarboxylase isolated from the strain *Saccharomyces cerevisiae* (YPDC,[1] EC 4.1.1.1) is an enzyme consisting of 4 identical subunits of 563 amino acids each. It performs the prototypical decarboxylation of 2-oxo acids using thiamin diphosphate (ThDP, the vitamin B1 coenzyme) and Mg(II) as cofactors and converts pyruvate to acetaldehyde in the penultimate step of alcohol fermentation (*1*−*6*). A minimal reaction mechanism according to the model first reported by Breslow (*7*) requires a number of steps with potential need for acid−base groups near the active center as seen in Scheme 1. An inspection of the X-ray structures of YPDC from *Saccharomyces uvarum* (*8*) and from *Saccharomyces cerevisiae* (*9*) indicates that aside from the amino group of the 4′-aminopyrimidine ring of ThDP, the reactive side chains of D28, H114, H115, and E477 are all within "striking" distance of the C2 atom of the thiazolium ring (Figure 1). These residues are potential candidates for converting the thiazolium C2H to the C2 carbanion/ylide to initiate the reaction. Systematic substitution at these positions provides the opportunity to elucidate the roles of these amino acids, if any, in catalysis. Optimally, a comparison of the pH dependence of the steady-state kinetic parameters for YPDC and variant enzymes may reveal not only whether such groups participate in a step reflected by the kinetic parameters, but also whether a particular group participates in its conjugate acid or conjugate base ionization state.

† This work was supported at Rutgers by NIH Grant GM-50380, NSF Training Grant BIR 94/13198 in Cellular and Molecular Biodynamics (F.J., PI), and the Rutgers University Busch Biomedical Fund and Roche Diagnostics Corp., Indianapolis, IN, at Halle by the Fonds of Chemical Industry, Germany and at Pittsburgh by NIH Grant GM-48195 and VA Merit Review 185-12-8499.

* To whom correspondence should be addressed. Tel: 973-353-5470, FAX: 973-353-1264, E-mail: frjordan@newark.rutgers.edu.

‡ Rutgers, The State University of New Jersey.

§ Martin-Luther-University.

⊥ University of Pittsburgh School of Medicine and the VA Medical Center Biocrystallography Laboratory.

[1] Abbreviations: ThDP, thiamin diphosphate; PDC, yeast pyruvate decarboxylase (EC 4.1.1.1); YPDC, pyruvate decarboxylase (WT) isolated from *Saccharomyces cerevisiae* and expressed in *E. coli*; ZmPDC, pyruvate decarboxylase from *Zymomonas mobilis*; D28A, D28N, H114F, H115F, and E477Q are variants at the indicated positions; SDS−PAGE, sodium dodecyl sulfate−polyacrylamide gel electrophoresis; IPTG, isopropyl-*β*-D-thiogalactopyranoside; PMSF, phenylmethanesulfonyl fluoride.

10.1021/bi002855u CCC: $20.00
Published on Web 06/02/2001

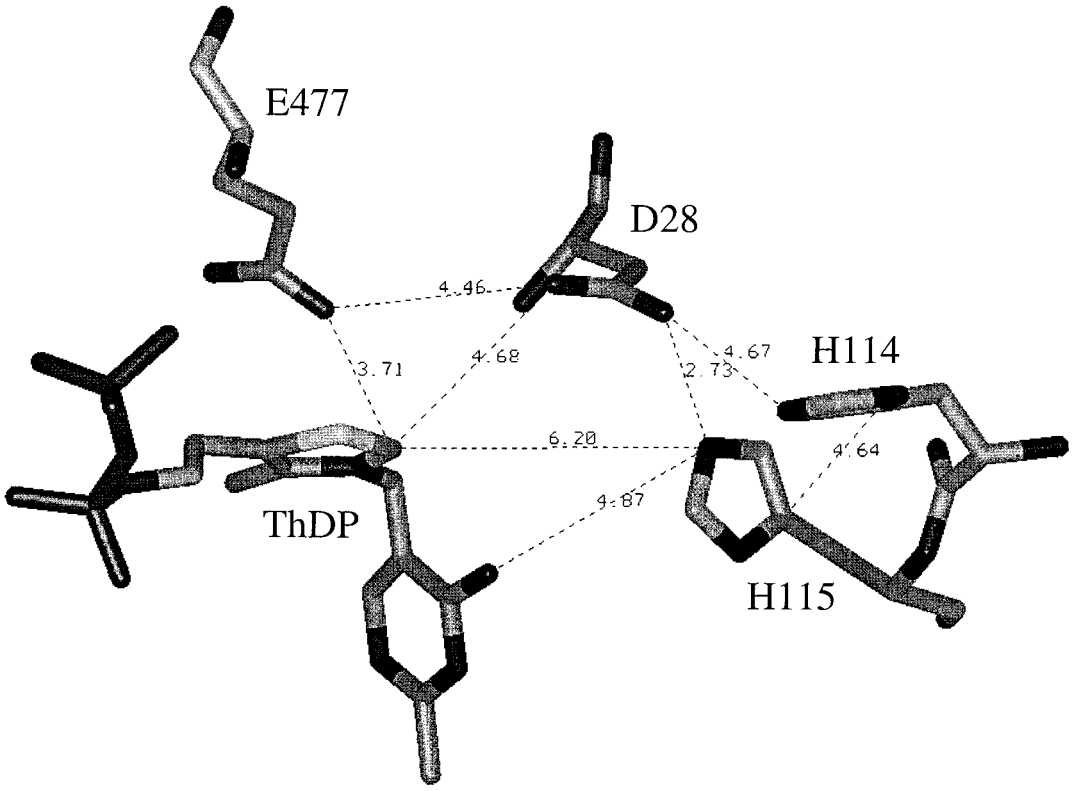

FIGURE 1: Location of residues D28, H114, H115, and E477 near ThDP (*9*).

Scheme 1

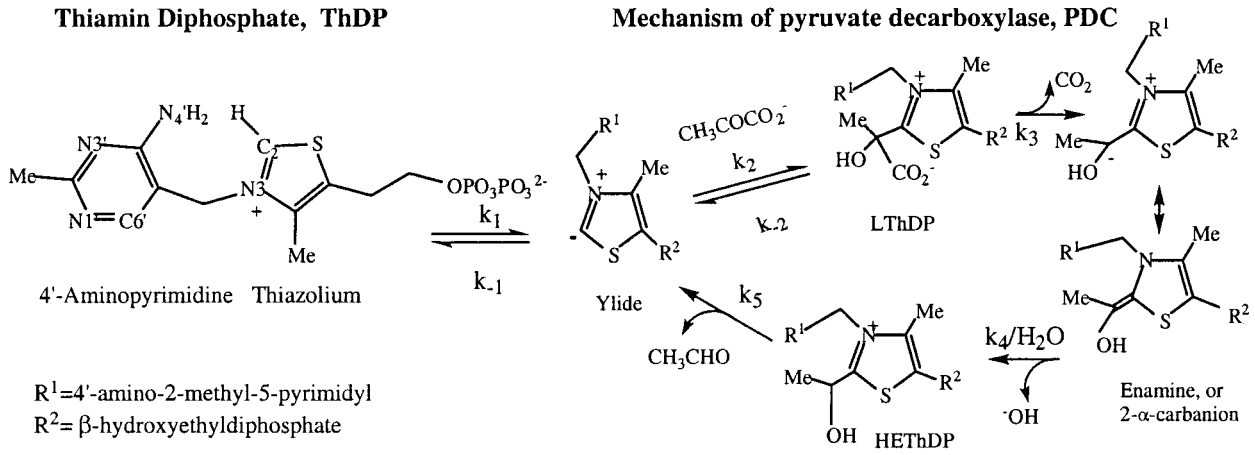

Although thiamin, indeed thiazolium salts, can also catalyze several reactions among those carried out by the enzymes at a very slow rate, the role of the amino acids surrounding the coenzyme during catalysis is still relatively unknown. Studies have been directed to Glu51 (*10*−*12*), a conserved amino acid present within a short hydrogen-bonding distance of the N1′ atom of the 4′-aminopyrimidine ring; Ile415 (*13*), whose hydrophobic side chain appears to be the conformational pivot which is helping to maintain the optimal 'V' conformation of the coenzyme; and a series of studies on the substrate regulatory site and pathway (*14*−*22*). It had been estimated (*23*) that compared to model ThDP reactions, the YPDC apo-protein accelerates the reaction by a factor of 10^{12}−10^{13}. It is of importance to understand the origins of this impressive rate acceleration. Since the pK_a of the thiazolium ring has been estimated to be between 17 and 19 in aqueous solution (*24*), one may surmise that substitution of the catalytic base responsible for converting the thiazolium ring to its conjugate base would have a dramatic effect on the rate of the reaction. On the basis of the published crystal structures, all of these amino acids have been mentioned as potential key catalytic bases (see preliminary results in ref *19* on YPDC, refs *25* and *26* on ZmPDC, and ref *27*, a modeling study based on YPDC coordinates).

We here report that all four amino acids are indeed involved in catalysis in some manner, affecting both k_{cat} and $k_{cat}/S_{0.5}$. Yet, since none of the substitutions leads to inactive enzyme, the magnitude of the reduction in k_{cat} and $k_{cat}/S_{0.5}$, while appropriate for a general acid−base group or a hydrogen-bonding interaction, does not suggest that any of the four groups participate in deprotonation of the thiazolium C2 atom as the initial step in catalysis. With some modest exceptions, nor do the substitutions lead to significant changes in the shape of the pH dependence of the steady-

state kinetic parameters. This latter finding is consistent with the notion that the state of ionization of these groups does not change during the rate-limiting step(s) or that the changes are concerted so as not to alter the overall electrostatics at the active center.

In the accompanying papers (*41, 42*), additional mechanistic tools are applied (*41*), and, on the basis of the novel kinetic behavior of some of these variants, a new, more complex mechanism is put forth for yeast pyruvate decarboxylase (*42*).

EXPERIMENTAL PROCEDURES

Materials. The T7 *E. coli* expression system was purchased from Novagen, Inc. *E. coli* DH5α strain and low melting point agarose were purchased from Life Technologies, Inc. The *pfu* DNA polymerase was from Stratagene, Inc. The following items and most of the restriction enzymes were purchased from Promega, Inc.: Wizard PCR product purification kit, Wizard plasmid mini-prep kit, 373 DNA sequencing plasmid prep kit, dNTPs. The DNA sequencing kit was purchased from Perkin-Elmer Corp. The nutrients of LB medium (Difco) were purchased from Fisher, Inc. Sephacryl S300 and DEAE Sephacel were from Phamacia, Inc. Hydroxylapatite (HTP) gel was purchased from Bio-Rad Laboratories.

Gene Cloning and Site-Directed Mutagenesis. The plasmids were prepared with the Promega Wizard mini-prep kit. DNA digestions with restriction endonucleases were performed according to the manufacturers' instructions. The DNA fragments were purified by low melting point agarose gel electrophoresis. The agarose gel slices containing the desired DNA fragments were melted by heating at 65 °C for 5 min. The DNA fragments were harvested from the melted agarose using the Promega Wizard PCR product purification kit. All ligation reactions were performed with T4 DNA ligase in 1× ligation buffer (provided by the manufacturer) at 16 °C for 10−12 h. The desired recombinant DNA plasmids were transformed with *E. coli* DH5α cells under antibiotic pressure (ampicillin at 50 mg/L of culture). The plasmids prepared from single colonies of *E. coli* DH5α transformants were further confirmed by genetic map analysis.

Mutagenesis was performed with the PCR megaprimer method (*28*). The PCR reactions were carried out with 25 thermocycles (92 °C for 2 min, 55 °C for 1 min, and 72 °C for 2 min) with a MiniCycle (MJ Research, Inc.) at conditions of 0.1 mg of template for PCR I and 1.0 mg of template for PCR II, 0.5 mg of oligodeoxynucleotide primers, 1× *pfu* polymerase buffer, 2.5 mM $MgCl_2$, 0.2 mM dNTPs, and 1 IU of *pfu* DNA polymerase. The primers used are listed below:

front flanking primer (T7 promoter primer):

5′-CCGCGAAATTAATACGACTCACTATA-3′

back flanking primer (T7 terminator primer):

5′-GTTATGCTAGTTATTGCTCAGAGGT-3′

The mutagenic primers were

5′-ACCCAAGGTGAAGTGCAACAACAATTGCTT-3′ for H115F

5′-GGTTACACCATCCAAAAGTTGATTCACGGT-3′ for E477Q

5′-GGTTACACCATCGATAAGTTGATTCACGGT-3′ for E477D

5′-GGTTACACCATCAATAAGTTGATTCACGGT-3′ for E477N

5′-GGTTTGCAAGGTGCATTCAACTTGT-3′ for D28A

5′-GGTTTGCCAGGTAACTTCAACTTGT-3′ for D28N

5′-ACCCAAGGTGTGGAACAACAACAATTGCTT-3′ for H114F

5′-ACCCAAGGTGAAGAACAACAACAATTGCTT-3′ for H114F/H115F

The mutations were confirmed by DNA sequencing using an ABI 373 DNA sequencing system with the PRISM Ready Reaction Dideoxy terminator cycle sequencing kit (Perkin-Elmer Corp.).

Design of C-Terminal His_6-tag for WT YPDC and Variant Proteins. In the pET-22b cloning/expression region, there is present the following DNA.

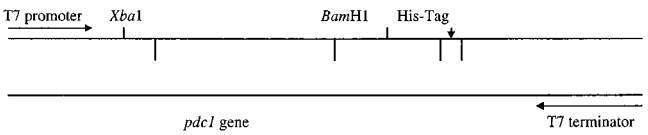

Following the *pdc1* gene, there are four stop codons (TAA). These are not consecutive, but are all within 60 base pairs of the *pdc1* gene. Immediately following the His_6-tag sequence, there is an additional stop codon (TGA). To express the gene with the His_6-tag attached, the four stop codons (TAA) must be either eliminated or replaced by non-stop codons. Since there are four such stop codons, it is difficult to use site-directed mutagenesis methods to mutate them. Instead, primer A was designed to eliminate all four stop codons. Primer A has the following sequence: 5′-CTGC GGATCC AG TTGCTTAGCGTTGGTAGCAGCAGT-3′.

Primer A is annealed to the template from the right-most (the first) stop codon (TAA), and toward the left in Scheme 2. It also contains a *Bam*HI cleavage site near the 5′-end. If the PCR reaction is carried out using the T7 promoter primer and primer A as the two primers, along with plasmid pET22b(+)-*pdc1* as the template, the DNA fragment shown in Scheme 3 will result, containing the *pdc1* gene and the *Xba*I and *Bam*HI cleavage sites, but not the four stop codons. Different versions (WT or mutants) of template plasmids will result in different versions of *pdc1* gene in the DNA fragment.

Finally, the DNA fragment, along with the WT plasmid pET22b(+)-*pdc1*, is digested with the two DNA restriction endonucleases, *Xba*I and *Bam*HI. The digested DNA fragment is then ligated to the larger part of the digested plasmid, which has the His_6-tag at its terminus. The final plasmid can be transformed with *E. coli* DH5α or *E. coli* BL21 cells, and then expressed with the C-terminal His_6-tag. This enzyme could be purified on a Talon affinity column (*29*).

Most importantly, the purified C-terminally His_6-tagged WT YPDC was kinetically indistinguishable from WT YPDC in every respect, including substrate activation (*30*).

Scheme 2

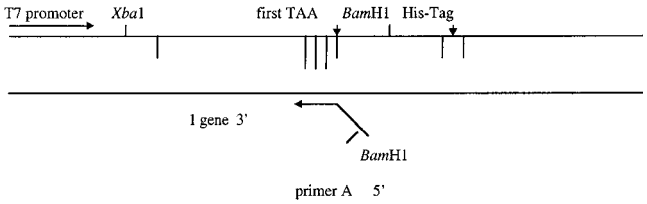

Scheme 3

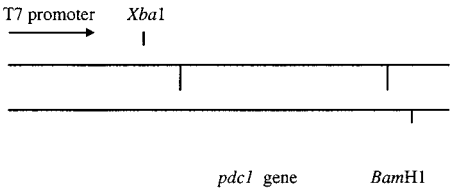

Protein Overexpression and Purification. All purification steps were carried out at 4 °C. The BL21 cells were grown in LB medium (containing 0.05 mg/mL ampicillin, 0.5 mM thiamin chloride, and 1 mM $MgCl_2$) at 37 °C with shaking at 300−325 rpm to an A_{600} of 1.0−1.2. The The cells were harvested and resuspended with 20 mM potassium phosphate buffer (pH 6.8) containing 0.5 mM EDTA-2Na, 2 mM $MgCl_2$, 1 mM PMSF, and 1 mM ThDP. The cell suspension was disrupted at 20 kHz for 4 min (with 10 s on, 10 s off) on a model 550 Sonic Dismembrator and then centrifuged at 18 000 rpm at 4 °C for 30 min. To the suspension was added ammonium sulfate to a final concentration of 1.5 M. The solution was then stirred for 15 min and then centrifuged for 15 min. The precipitate was discarded, and to the supernatant was added ammonium sulfate, this time to a final concentration of 2.8 M with continuous stirring for 15 min. The pellet containing the crude enzyme was collected by centrifugation for 15 min. The pellet was resuspended in 20 mM Bis-Tris buffer (pH 6.8) containing 0.5 mM EDTA-2Na, 2 mM $MgCl_2$, 0.5 mM PMSF, and 1 mM ThDP and then dialyzed against the same buffer at 4 °C overnight. The desalted protein solution was filtered through a 0.2 μm syringe filter and loaded onto an Pharmacia HiLoad Q Sep (HP) column (26 mm × 100 mm) equilibrated with 20 mM Bis-Tris (pH 6.8) containing 0.5 mM EDTA-2Na and 2 mM $MgCl_2$. The protein was eluted by a linear gradient with 2 M NaCl at a flow rate of 5.0 mL/min. The gradient was carried out with the FPLC director computer program (Pharmacia).

The fractions were collected in glass tubes containing 1 mM ThDP. Enzyme activity and protein content were measured for each fraction, and the purity was checked using SDS−PAGE. The purified sample was concentrated with a Centriprep-30 concentrator device by centrifugation at 5000 rpm at 4 °C until the sample volume was reduced to about 500 μL. The concentrated sample was then added to 3 mL of 100 mM NaH_2PO_4 buffer (pH 6.0) containing 1 mM $MgCl_2$ and 1 mM ThDP, and then centrifuged at 5000 rpm at 4 °C for 20 min. The cycle of buffer addition followed by concentration was repeated 2 more times. For long-term storage, glycerol was added to the preparation to a final concentration of 50% (v/v), and the enzyme was stored at −20 °C.

Protein concentration was determined with the Bio-Rad protein assay dye reagent (Bradford method) (*31*). The purity and yield of each variant were judged by SDS−PAGE.

Scheme 4

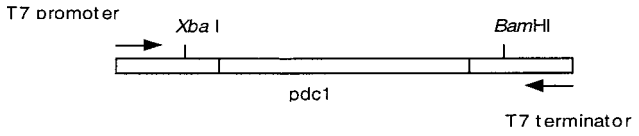

Activity and Kinetic Measurements. YPDC activity was assayed with the NADH/alcohol dehydrogenase (ADH) coupled assay, converting the acetaldehyde to ethanol and monitoring the depletion of NADH at 340 nm (*32*). One unit of YPDC activity is defined as the amount of protein required to convert 1.0 μmol of pyruvate to acetaldehyde per minute at 25 °C. The kinetic studies were carried out on a Cobas-Bio centrifugal analyzer (Roche Diagnostic Systems). The kinetic parameters were calculated by curve fitting using the Sigma-plot program from SPSS.

The pH-dependent steady-state kinetic studies were carried out in a triple buffer consisting of 50 mM MES, 100 mM Tris, and 50 mM acetic acid, along with 1 mM $MgCl_2$, 1 mM ThDP, and 0.2 mM EDTA-Na_2 (henceforth 'standard buffer'). The standard buffer was then adjusted to the desired pH. This combination of three buffers has the advantage of providing a constant ionic strength in the entire pH range studied (*33*). Aware of some reports criticizing the use of Tris with alcohol dehydrogenase-linked assays (*34, 35*), we carried out several control experiments showing that at pH 7.5 (the highest pH used in this paper), or lower, substitution of *N*-ethylmorpholine (a tertiary amine) for Tris (a primary amine attached to a tertiary carbon) makes no difference in the steady-state kinetic parameters (tested at pH 6.0 and 7.5). Although citrate has been often used for this enzyme, both its variable ionic strength in the pH range of interest and its identification at several locations in a recent pyruvate decarboxylase structure (*39*) make its use over a wide pH range questionable. At the same time, due to the charges present in all key intermediates (and associated transition states), use of a constant ionic strength is deemed essential.

Determination of the State of Carbon Dioxide Generated by a Continuous Kinetic Assay. The details of the continuous carbon dioxide kinetic assay will be described elsewhere. Briefly, the end-point-coupled enzymatic assay for the determination of bicarbonate ion sold by Sigma was adapted with slight modifications to enable continuous monitoring of bicarbonate formation. WT and the D28A and E477Q variants were each assayed in the presence and absence of carbonic anhydrase.

Determination of the C2 H/D exchange rates of bound ThDP was carried out by a published method validated on several ThDP enzymes at the Halle laboratories (*11*).

RESULTS AND DISCUSSION

DNA Protocols. The recombinant plasmid pET22b(+)-*pdc1* was constructed to resemble pET1120-*pdc1* (*36*). The cloned 1 gene is flanked by certain genetic features (Scheme 4), allowing the PCR products carrying the desired mutation points to be cloned back into pET22b(+) at the *Xba*I and *Bam*HI restriction sites. All mutations were confirmed by DNA sequencing.

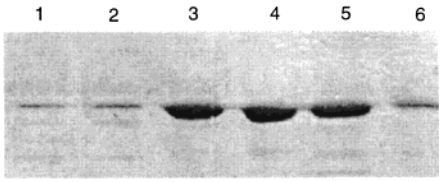

FIGURE 2: Typical SDS−PAGE analysis for the purification of the H114F YPDC variant. Bands 1−6 are fractions collected from the Hiload (26/100 mm) Q Sepharose high performance column.

Protein Purification. The initial purification protocol used for the variant proteins produced in *E. coli* cells was a modified version of that for enzyme isolated from yeast (*37*). This protocol, with a series of steps including heat treatment of the *E. coli* crude extract to 50 °C, followed by a sequence of DEAE Sephacel and hydroxylapatite gradient chromatography, yields WT YPDC with a specific activity of 55 IU/mg of protein. SDS−PAGE shows a single protein band with molecular mass of 62 kDa (see Figure 2 for illustration with the H114F variant purified by the FPLC method) with a yield of 100−200 mg of *E. coli* culture. The typical DEAE chromatographic procedure appeared to inactivate all of the active center variants. When purified to lesser purity, these enzyme variants showed activity, but eventually we found that some of the activity was independent of the presence of ADH, signaling some hitherto unidentified activity that becomes important especially with the low-activity variants.

Control experiments were carried out to show that when ADH was incubated in the pH range of 4.6−7.8 for 5 min prior to measurement at pH 6.0, the YPDC activity was unaffected. Nor was the YPDC activity affected when ADH was preincubated at pH 5.0 and 6.0 for 30 min prior to the assay. These tests showed that under the experimental conditions, ADH is stable.

According to our experiments, the interference also resulting in loss of pyruvate and depletion of the NADH absorption at 340 nm (even in the absence of ADH) is due to endogenous lactate dehydrogenase present in the *E. coli.* Once this issue was recognized, an FPLC method was developed that could successfully separate ADH-dependent and ADH-independent activities in the YPDC assay; the ADH-independent activity is in a totally different peak in the chromatogram (data not shown). The WT and the E477Q variant are also available as their C-terminally His_6-tagged analogues, in which case affinity chromatography on a Talon chelate column could also separate the YPDC from the lactate dehydrogenase contamination. Typically, the WT had less than 1% interference and the variants 3−5% ADH-independent activity vs 95−97% ADH-dependent ('true') activity. This issue turned out to be very important for all of the active center derivatives, where the activity is reduced by at least 100-fold. The limited preliminary results reported several years ago (*19*) were obtained on partially purified enzymes. While the general picture has changed little, the numbers reported below indicate that these substitutions damaged the enzyme even more than reported earlier.

Steady-State Kinetic Analysis of the WT YPDC and Variant Enzymes. The steady-state kinetic parameters were determined in the pH range of 5.0−7.5 on the wild-type and most variants by adjusting the pH of the triple standard buffer (see Experimental Procedures) to the desired value with strong acid or base. The WT YPDC is an allosteric enzyme; it exhibits sigmoidal v_0−[S] profiles. It is also susceptible to inhibition at high substrate concentrations, an inhibition that varies with the substitution. The data were analyzed according to the Hill treatment in eq 1, where v_0 is the initial velocity, $[E_0]$ is the total enzyme concentration, k_{cat} is the turnover number, [S] is the substrate concentration, $S_{0.5}$ is the substrate concentration when v_0 is half of the maximal velocity, K_i is the dissociation constant for the enzyme−substrate inhibitory complex, and n_H is the Hill coefficient. The pH profiles of these parameters on the WT YPDC and the D28A, H114F, H115F, and E447Q variants are shown in Figures 3−7 and Tables 1−5.

$$v_0/[E_0] = k_{cat}[S]^n/\{S_{0.5}{}^n + [S]^n(1 + [S]/K_i)\} \quad (1)$$

The data were also analyzed using eq 2, formalism derived by Schellenberger, Hübner, and Schowen (SHS) and their co-workers (*23*), where the initial velocity−substrate concentration plots are divided into three regions, yielding three rate constants: k_{cat}/A (second order in substrate at substrate concentrations tending to 0), k_{cat}/B (first order in substrate at intermediate substrate concentrations), and k_{cat} (zero order in substrate; valid at high substrate concentrations).

$$v_0/[E_0] = k_{cat}[S]^2/\{A + B[S] + [S]^2(1 + [S]/K_i)\} \quad (2)$$

Hence, the smallest unit to be considered, the monomer, may bind as many as two substrate molecules, accounting for a Hill coefficient of less than 2.0. The calculated steady-state kinetic parameters for all YPDC species reported here are listed in Tables 1−5. It is important to note at the outset that the SHS data treatment did not turn out to be useful for several of the conditions and variants used [addressed in detail in paper 3 (*42*) of this series]. While the SHS treatment would be advantageous for this allosteric enzyme, so that the regulatory and catalytic centers could be identified, the properties of the variants did not enable us to use the SHS data treatment for the most part. Apart from that, we had to rely on the quantity $k_{cat}/S_{0.5}$, a quantity that is a weighted average of k_{cat}/A and k_{cat}/B in the SHS treatment. In addition, we also generated $k_{cat}/S_{0.5}{}^n$−pH plots (from the Hill treatment), a function that better approximates k_{cat}/A in the SHS treatment, encompassing transition states from the addition of the first substrate to the free enzyme through the first irreversible step, decarboxylation. In the third paper of this series (*42*), we reconsider this entire issue in detail.

Effects of Substitution on k_{cat}. Compared to the wild-type YPDC, substitutions at all four residues reduce the k_{cat} by 400−1000-fold. Therefore, all four residues are involved in the mechanism, and all help to stabilize transition states in step(s) commencing with the first irreversible step, decarboxylation. The shape of the k_{cat}−pH curves is similar in the substituted enzymes to that for the wild-type YPDC, with only relatively small perturbations in the apparent pK_a's (see Table 6). The apparent pK_a at the acid side is more reproducible, and is present in all enzyme forms. There appears to be a small shift to higher apparent pK_a in the D28A plots, and to a lesser extent in the H115F plots, while the plots of the H114F and E477Q variants are unchanged compared to the WT enzyme. There is a hint in the behavior

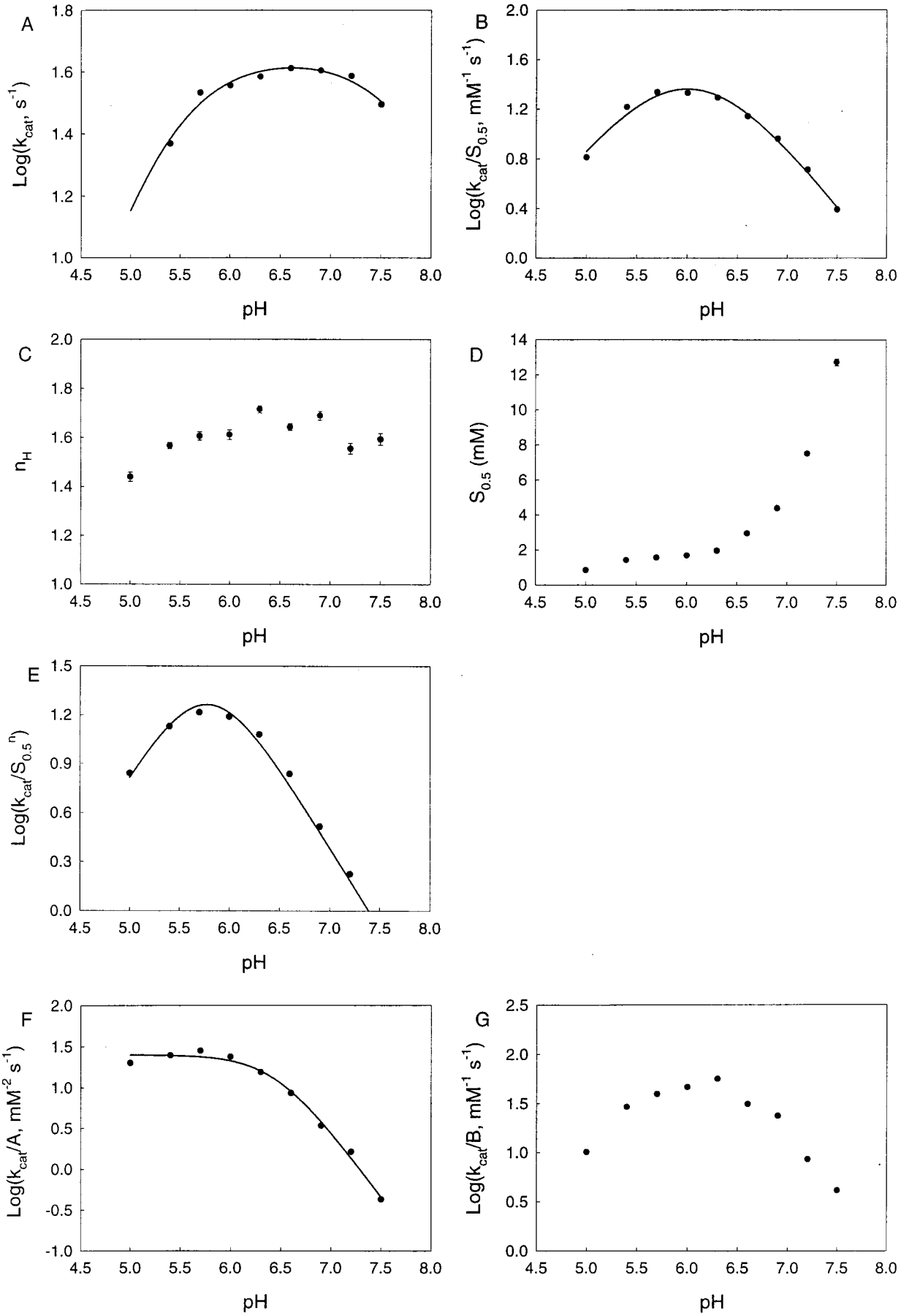

FIGURE 3: pH dependence of the steady-state kinetic parameters of WT YPDC. (A) Dependence of log(k_{cat}) on pH. (B) Dependence of log($k_{cat}/S_{0.5}$) on pH. (C) Dependence of n_H on pH. (D) Dependence of $S_{0.5}$ on pH. (E) Dependence of log($k_{cat}/S_{0.5}^{n}$) on pH. (F) Dependence of log(k_{cat}/A) on pH. (G) Dependence of log(k_{cat}/B) on pH.

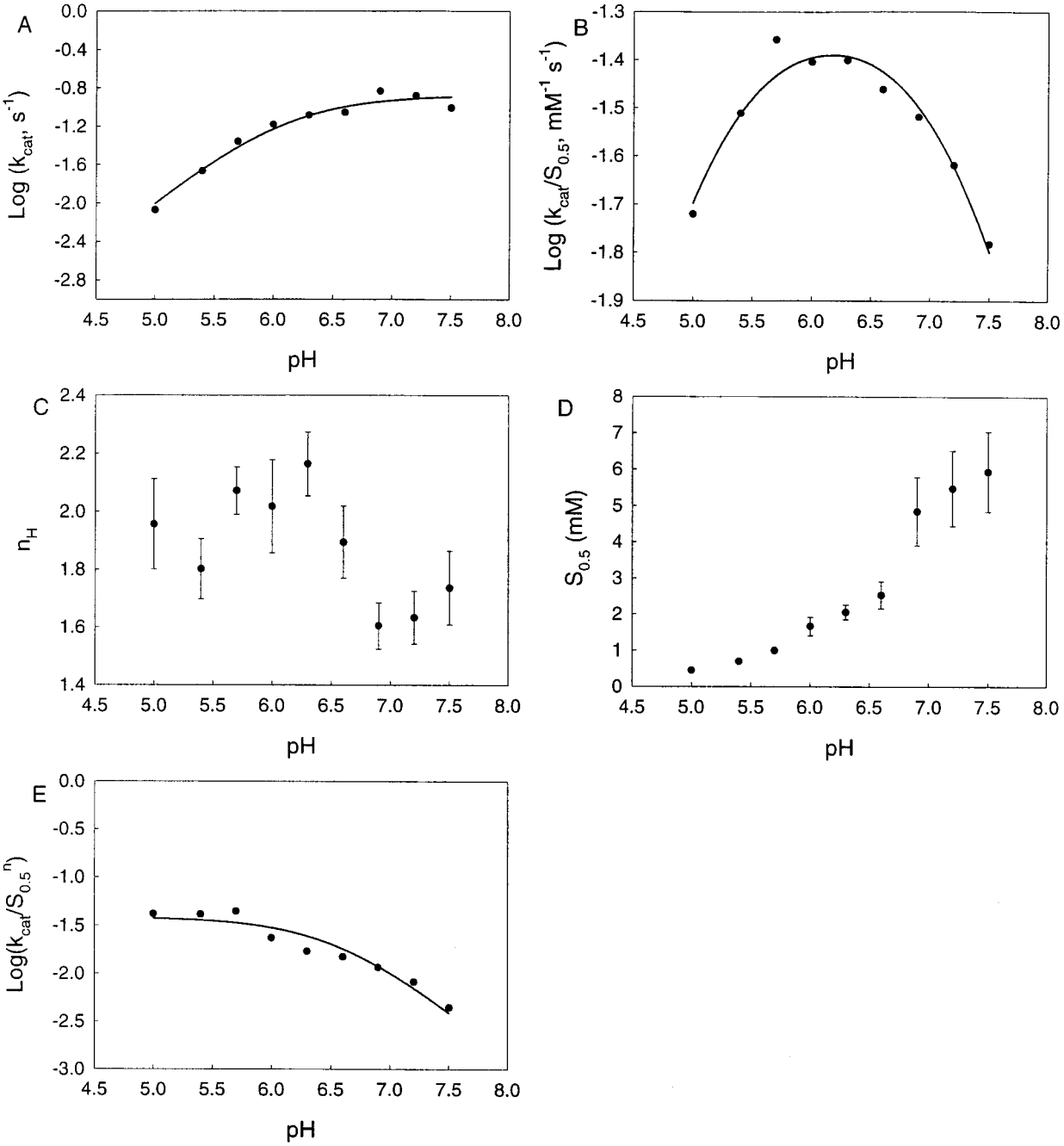

FIGURE 4: pH dependence of the steady-state kinetic parameters of D28A YPDC. (A) Dependence of log(k_{cat}) on pH. (B) Dependence of log($k_{cat}/S_{0.5}$) on pH. (C) Dependence of n_H on pH. (D) Dependence of $S_{0.5}$ on pH. (E) Dependence of log($k_{cat}/S_{0.5}^{n}$) on pH.

of the D28A and H115F plots that residues D28 and H115 act in unison, and affect each other, not surprising in view of the hydrogen bond between these side chains implied by the X-ray structure (see Figure 1). The results suggest that for stabilizing the rate-limiting transition state at high substrate concentration, some residue(s) in its conjugate base form is (are) required, and, while the H115F and D28A substitutions are not fatal to the activity, the optimal activity is only achieved at higher alkalinity than in the wild-type enzyme. This would be consistent, for example, with a dissociated form of D28 being needed post-decarboxylation, as also implied by the carboligase side reaction in paper 2 (*41*) of this series.

The modest decrease in activity at higher pH (>7.0) is real, but the pH range of activity studied does not enable accurate determination of this pK_a.

Effects of Substitution on $k_{cat}/S_{0.5}$ and Related Constants. This rate constant is usually interpreted as the 'catalytic efficiency' of the enzyme and incorporates transition states culminating with the first irreversible step, in this case decarboxylation. First of all, all $k_{cat}/S_{0.5}$−pH profiles are bell-shaped for both wild-type and YPDC variant enzymes. This behavior has not always been appreciated in previous studies of YPDC, and has been reported to have very different pH dependence in ZmPDC (*26*). At the pH optima for the $k_{cat}/S_{0.5}$−pH curve, the catalytic efficiency of the variants is ca. 1000−3000 lower than that of the wild-type YPDC. Again, as with the k_{cat} values, all four residues tested appear to have involvement in lowering the energy of the rate-limiting step-(s) culminating in decarboxylation, i.e., at low substrate

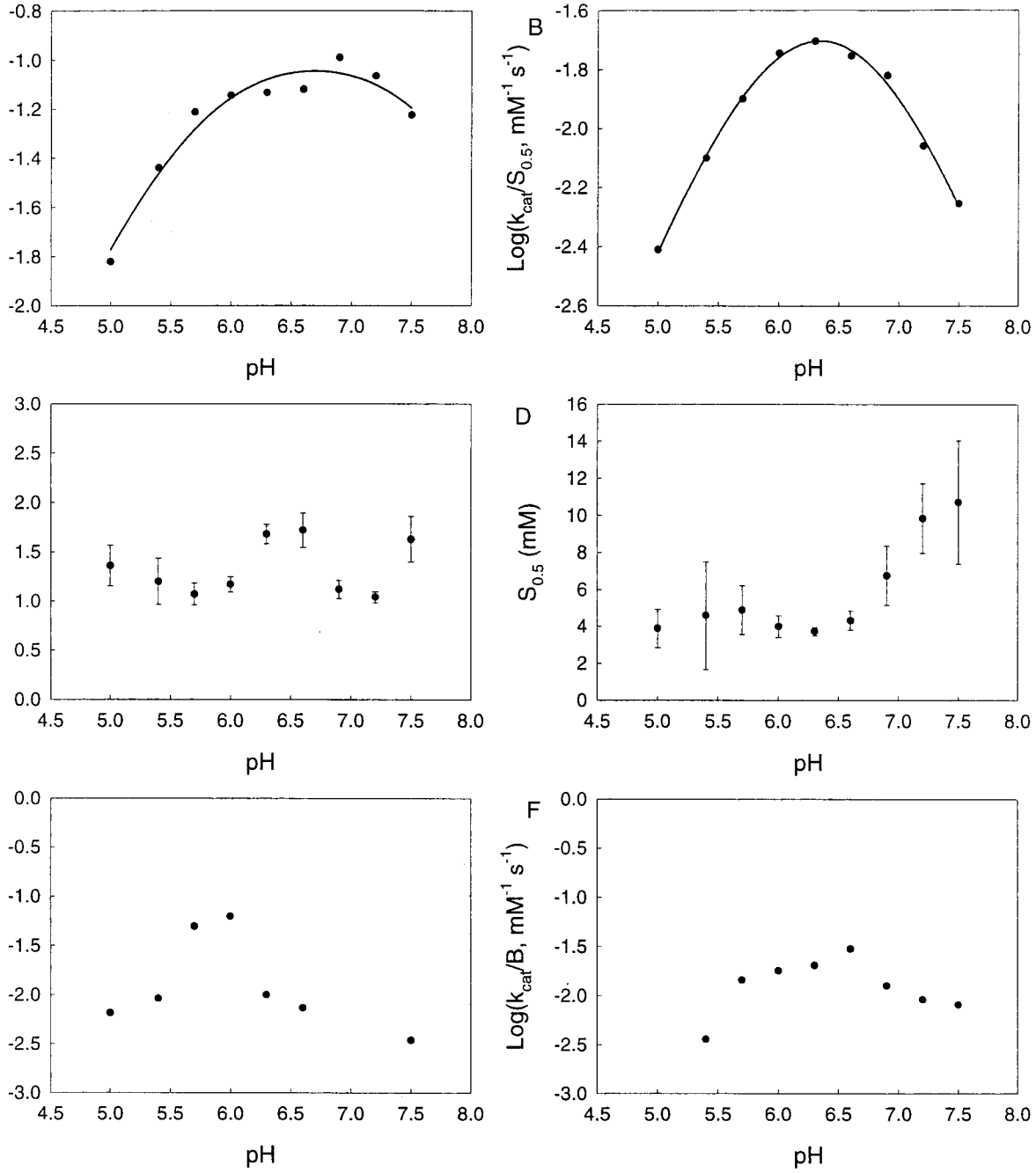

FIGURE 5: pH dependence of the steady-state kinetic parameters of H114F YPDC. (A) Dependence of log(k_{cat}) on pH. (B) Dependence of log($k_{cat}/S_{0.5}$) on pH. (C) Dependence of n_H on pH. (D) Dependence of $S_{0.5}$ on pH. (E) Dependence of log(k_{cat}/A) on pH. (F) Dependence of log(k_{cat}/B) on pH.

concentrations, where interactions of substrate with the free enzyme or with the substrate-activated enzyme are dominant.

It is relevant to mention as well, that while the quantity $S_{0.5}$ is difficult to interpret, its magnitude (in general, it tends to lower values with decreasing pH) is much larger for H114F than for H115F, two variants which in turn have larger values than those for the E477Q and D28A variants (the latter is the smallest of the four, approaching values for the wild-type enzyme). Given that the likely regulatory site (C221) is at least 20 Å from these residues, the pH dependence of these constants is most probably modulated by charges at the catalytic center. The results suggest that through the decarboxylation step, the charges at the two His are more important for substrate binding than the charges at D28 or E477, as also suggested for the corresponding residues in ZmPDC (*26*).

As can be seen in the figures and tables, the SHS formulation works well for the wild-type YPDC near the pH optimum, and for the H114F and H115F variants, providing bell-shaped k_{cat}/A−pH, k_{cat}/B−pH, or $k_{cat}/S_{0.5}$−pH plots. However, with the E477Q and D28A variants, we could not fit the data in any meaningful way according to this kinetic formulation [see paper 3 (*42*) in this series], yet the $k_{cat}/S_{0.5}$−pH plots are bell-shaped even for these variants.

Some interesting, more subtle changes are in evidence in the various plots.

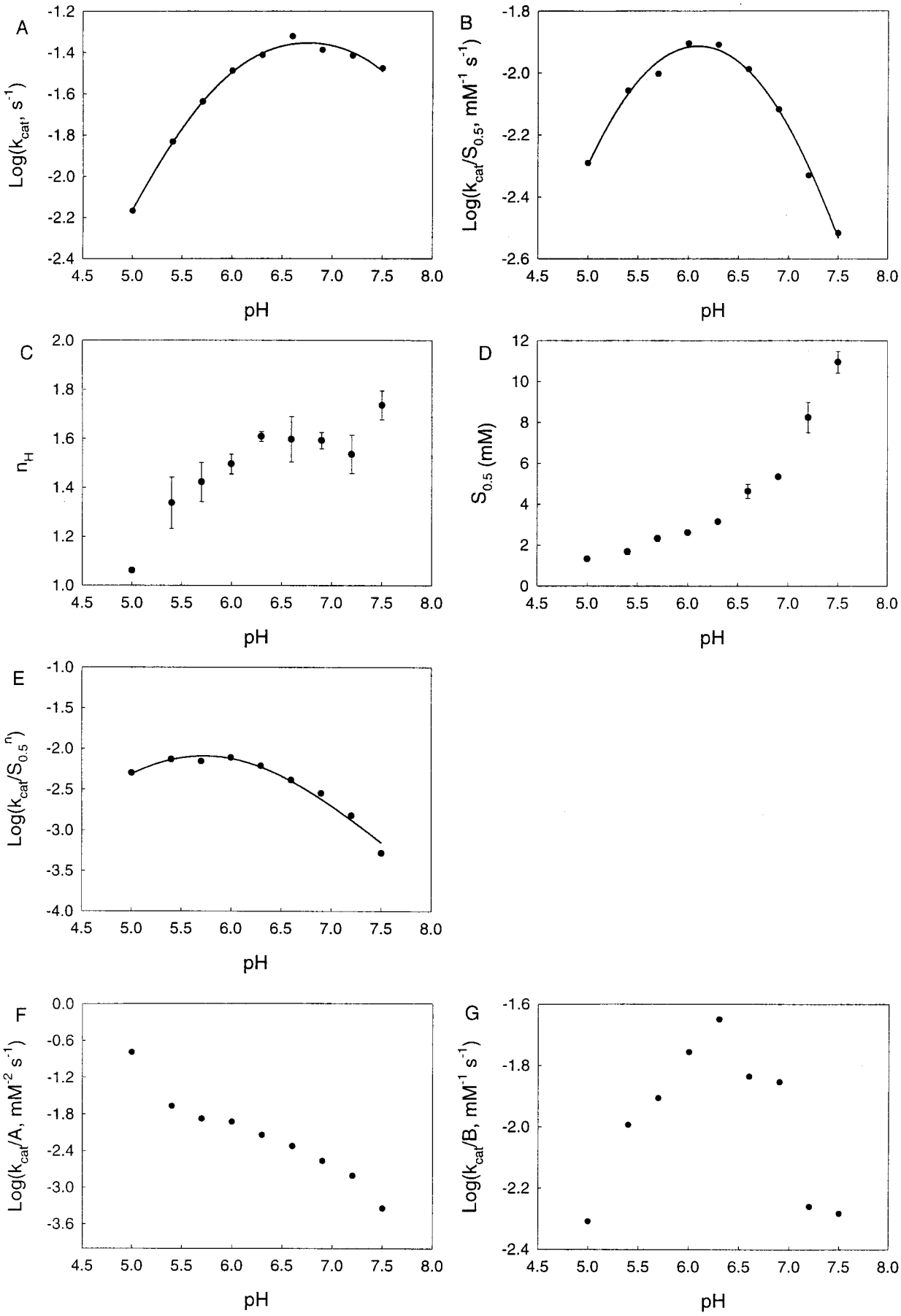

FIGURE 6: pH dependence of the steady-state kinetic parameters of H115F YPDC. (A) Dependence of log(k_{cat}) on pH. (B) Dependence of log($k_{cat}/S_{0.5}$) on pH. (C) Dependence of n_H on pH. (D) Dependence of $S_{0.5}$ on pH. (E) Dependence of log($k_{cat}/S_{0.5}^{n}$) on pH. (F) Dependence of log(k_{cat}/A) on pH. (G) Dependence of log(k_{cat}/B) on pH.

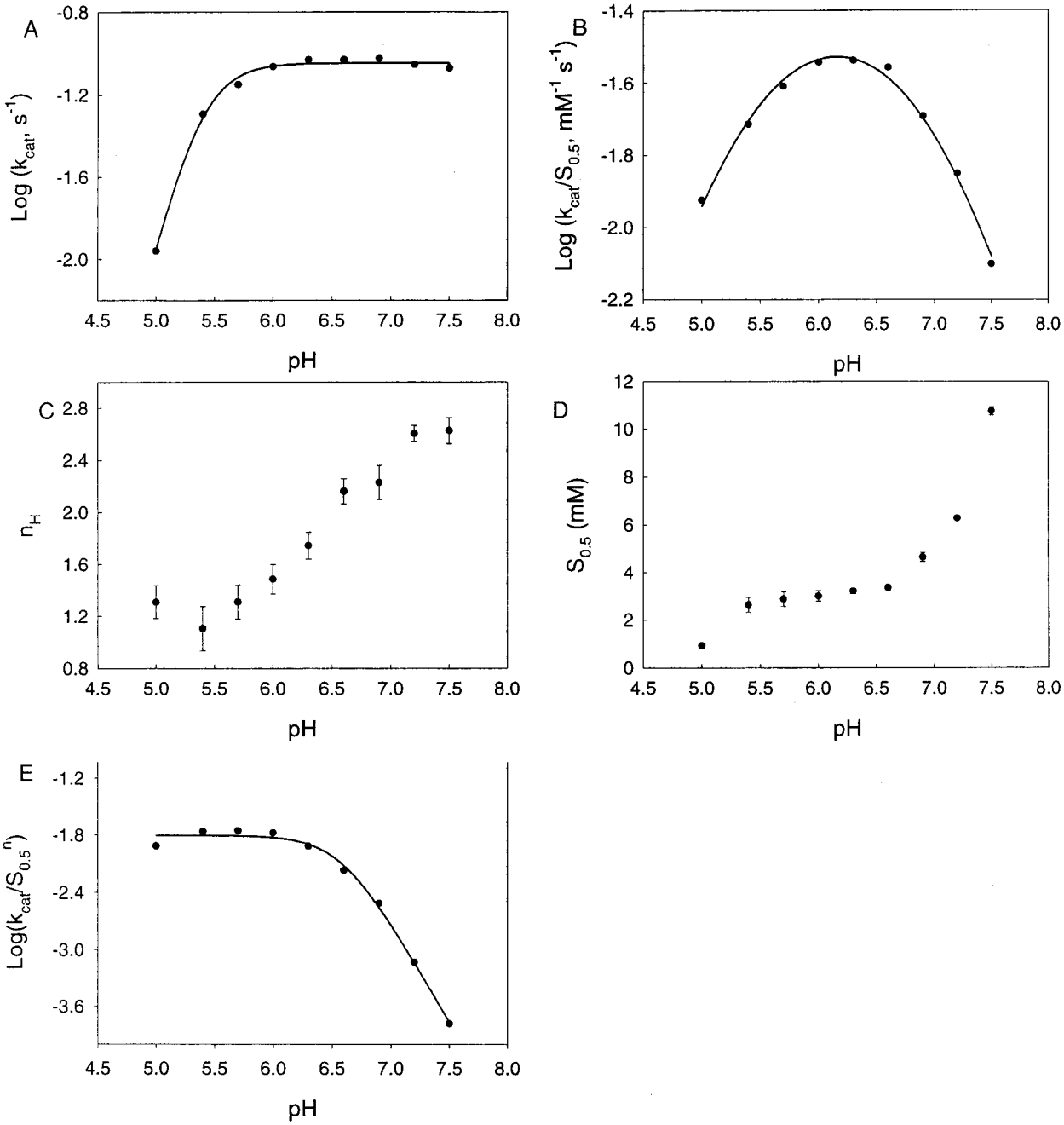

FIGURE 7: pH dependence of the steady-state kinetic parameters of E477Q YPDC. (A) Dependence of log(k_{cat}) on pH. (B) Dependence of log($k_{cat}/S_{0.5}$) on pH. (C) Dependence of n_H on pH. (D) Dependence of $S_{0.5}$ on pH. (E) Dependence of log($k_{cat}/S_{0.5}^{n}$) on pH.

Table 1: Steady-State Kinetic Parameters for Wild-Type YPDC

pH	k_{cat} (s^{-1})	$S_{0.5}$ (mM)	$k_{cat}/S_{0.5}$ (mM^{-1} s^{-1})	n_H	K_i (mM)	k_{cat}/A (mM^{-2} s^{-1})	k_{cat}/B (mM^{-1} s^{-1})
5.0	5.50 ± 0.14	0.85 ± 0.043	6.46 ± 0.36	1.44 ± 0.019	132.5 ± 20.1	20.12 ± 4.29	10.09 ± 2.19
5.4	23.37 ± 0.36	1.42 ± 0.044	16.45 ± 0.57	1.55 ± 0.013	389.4 ± 74.1	24.95 ± 2.22	29.07 ± 4.22
5.7	34.09 ± 0.46	1.57 ± 0.042	21.67 ± 0.66	1.60 ± 0.017	638.6 ± 161.1	28.15 ± 1.49	39.47 ± 3.75
6.0	36.02 ± 0.33	1.69 ± 0.044	21.30 ± 0.58	1.61 ± 0.020		23.66 ± 1.51	46.35 ± 5.08
6.3	38.42 ± 0.31	1.97 ± 0.046	19.50 ± 0.49	1.72 ± 0.015		15.39 ± 0.95	56.14 ± 8.83
6.6	40.96 ± 0.32	2.96 ± 0.065	13.84 ± 0.32	1.64 ± 0.014		8.57 ± 0.46	31.22 ± 3.03
6.9	40.20 ± 0.39	4.40 ± 0.11	9.13 ± 0.24	1.69 ± 0.018		3.41 ± 0.28	23.62 ± 4.21
7.2	38.67 ± 0.23	7.51 ± 0.098	5.14 ± 0.075	1.56 ± 0.021		1.62 ± 0.085	8.49 ± 0.54
7.5	31.28 ± 0.25	12.72 ± 0.18	2.46 ± 0.041	1.59 ± 0.023		0.42 ± 0.021	4.07 ± 0.32

With the wild-type YPDC, a superposition of k_{cat}/A−pH, k_{cat}/B−pH onto the $k_{cat}/S_{0.5}$−pH plot shows that the pH optimum of the $k_{cat}/S_{0.5}$−pH plot is between the pH optima of the k_{cat}/A−pH and k_{cat}/B−pH plots. The optimum of the k_{cat}/A−pH plot is to the acid side of that of the $k_{cat}/S_{0.5}$−pH plot, while the optimum of the k_{cat}/B−pH plot is slightly to the alkaline side of the optimum of the $k_{cat}/S_{0.5}$−pH plot. This is indeed one of the successes of the SHS formulation, and we believe that the pK_a's implicated by the k_{cat}/A−pH plot probably include ionization of C221 on the acid limb

Table 2: Steady-State Kinetic Parameters for the D28A Variant of YPDC

pH	$k_{cat} \times 10^3$ (s^{-1})	$S_{0.5}$ (mM)	$k_{cat}/S_{0.5} \times 10^3$ ($mM^{-1}\ s^{-1}$)	n_H	K_i (mM)
5.0	8.4 ± 0.2	0.44 ± 0.02	19.1 ± 1.3	1.95 ± 0.15	35.0 ± 9.6
5.4	21.0 ± 1.1	0.69 ± 0.04	30.4 ± 3.5	1.80 ± 0.10	4.6 ± 0.8
5.7	44.5 ± 2.1	0.99 ± 0.04	44.9 ± 4.1	2.07 ± 0.08	3.6 ± 0.3
6.0	66.2 ± 11.0	1.66 ± 0.25	39.9 ± 13.0	2.01 ± 0.16	3.0 ± 0.9
6.3	82.0 ± 10.0	2.06 ± 0.20	39.8 ± 8.6	2.16 ± 0.11	3.8 ± 0.8
6.6	88.3 ± 14.0	2.53 ± 0.37	34.9 ± 11.0	1.89 ± 0.12	5.2 ± 1.6
6.9	147.0 ± 28.0	4.84 ± 0.93	30.3 ± 12.0	1.60 ± 0.08	4.1 ± 1.2
7.2	132.2 ± 24.0	5.47 ± 1.03	24.2 ± 8.8	1.63 ± 0.09	7.1 ± 2.2
7.5	98.1 ± 16.0	5.93 ± 1.09	16.5 ± 5.7	1.73 ± 0.12	19.6 ± 9.2

and of H92 on the alkaline limb, the two residues that create the regulatory trigger, with approximate pK_a's of 5.2 and 6.4, respectively (*16*, *17*). At the same time, the pK_a's implied by the k_{cat}/B−pH plot must pertain to some other residues at the catalytic center, such as one of the four studied here or, perhaps, E51 and the proton relay from E51 to the thiazolium C2 position via the aminopyrimidine ring.

With the D28A variant, there appears to be no change in the $k_{cat}/S_{0.5}$−pH plot compared to wild-type YPDC, implying that D28 may be in its undissociated state through decarboxylation, a suggestion nicely borne out by the results of the carboligase studies in the second paper of this series (*41*). For the three other variants, H114F, H115F, and E477Q, there is an alkaline shift of the entire $k_{cat}/S_{0.5}$−pH bell-shaped curve, by approximately 0.2−0.4 unit, suggesting that (a) alteration of these potentially ionizable side chains produces similar effects, and at least one or more may bear a charge through the decarboxylation step, and (b) there is some important charge compensation accompanying any change on either acid or alkaline limb of the profile by a corresponding change on the other limb (otherwise, only one limb of the profile should be affected by a single substitution). One could envision an +/− interaction, in which elimination of one of the charges changes the pK_a of the remaining group, effectively neutralizing it in the pH region of interest.

Yet a different plot of the data, $k_{cat}/S_{0.5}^n$−pH, provides results analogous to the k_{cat}/A−pH plot in the SHS formulation. These plots are superimposable for wild-type YPDC and variants, with the exception of the D28A variant, which appears to experience a shift to the acid side. This appears to be the first hint that at least at low pH, D28 is involved significantly in a variety of ways in the mechanism. A very important implication from these profiles is that the effect of D28 substitution shifts the $k_{cat}/S_{0.5}^n$−pH curve and the k_{cat}−pH curves in opposite directions, suggesting that there is a change of ionization pre- and post-decarboxylation.

Effects of Substitution on the Hill Coefficient. In a series of papers from this laboratory (*14*−*22*), data have been summarized supporting the thesis that C221 (one of only four cysteines in yeast YPDC, the others being C69, C152, and C222) is the site where the substrate activation cascade is triggered. Successive substitutions of C221 on the β domain (and C222 to rule that residue out), H92 and E91 (both on the α domain), and W412 (on the γ domain) have suggested that this is the pathway along which information is propagated, with W412 affecting the adjacent G413, whose main chain carbonyl oxygen forms one of the conserved hydrogen bonds to the 4′-aminopyrimidine ring, which, according to our current working hypothesis, participates in crucial proton transfers during the reaction cycle.

The Hill coefficient as a function of pH is presented for the wild-type and variant YPDCs. For the wild-type YPDC and D28A and H115F variants, the Hill coefficients exhibit similar pH behavior, with the maximum value near 1.6−2.0. At the same time, for the E477Q variant the Hill coefficient rises to above 2.0 at higher pH values [a possible explanation for this observation will be put forth in the accompanying papers (*41*, *42*)]. The Hill coefficient for the H114F variant is definitely on the low end, only barely above 1.1 at nearly all pH values (in one of two complete pH runs, it was never higher than 1.2). For this H114F variant as well, the $S_{0.5}$ is at least 3 mM (for this variant, with a Hill coefficient of nearly 1.0, $S_{0.5}$ is essentially equal to K_m), higher than for the wild-type YPDC and the other variants studied here.

Also, for both wild-type and variant enzymes, the $S_{0.5}$ diminishes with decreasing pH, indicating that most likely both substrate molecules (at the regulatory and at the catalytic site) bind more firmly at lower pH. This pH behavior of $S_{0.5}$ in turn accounts for the bell-shaped $k_{cat}/S_{0.5}$−pH and related profiles.

Effects of Substitution on Substrate Inhibition. While all YPDC variants and wild-type enzyme exhibit at least a modest inhibition at high substrate concentrations (also pH dependent), of the enzyme forms studied here, the D28A variant exhibits as low as 3 mM K_i values. There may be several reasons for this behavior, and, as will be reported in the next paper (*41*), this is the only enzyme form that gives rise to a significant amount of acetolactate, one of the 'carboligase' side products (the carboligase side reaction occurs when the enamine intermediate can be trapped by electrophiles other than H^+, such as the substrate and the product of the YPDC reaction). It will also be shown, however, that the apparent substrate inhibition is not fully accounted for by the carboligase side reactions; rather, it is signaling the presence of several enzyme forms with activity.

Release of CO_2 by WT YPDC and the D28A and E477Q Variants. WT YPDC and the D28A and E477Q variants were tested to determine which form of carbon dioxide (CO_2 or HCO_3^-) is being produced at the active center. This is of importance for several reasons. The residues D28 and E477 are located proximal to the catalytic C2 of ThDP, and there is at least the possibility that they could catalyze such hydration reactions. The stoichiometry of the YPDC reaction near the pH optimum of 6.0 is: $CH_3COCOO^- + H_2O \rightarrow CH_3CHO + CO_2 + HO^-$; one would like to identify at which step the HO^- is released.

The curves for the time dependence of the release of carbon dioxide by WT YPDC and the D28A and E477Q variants were different in the presence and absence of carbonic anhydrase. The curves measured in the absence of carbonic anhydrase were characterized by a pronounced lag phase, which disappeared upon addition of excess carbonic anhydrase (data not shown).

From the effect of carbonic anhydrase on the coupled assay for bicarbonate determination, we could conclude that WT YPDC and the D28A and E477Q variants release carbon dioxide as a gaseous product. Omitting carbonic anhydrase from the assay resulted in a lag phase due to the slow rate of uncatalyzed (or 'spontaneous') hydration of the product. The first-order rate constant to reach the steady-state rate is 0.025 s^{-1}, a value comparable to the 0.04 s^{-1} rate constant

Table 3: Steady-State Kinetic Parameters for the H114F Variant of YPDC

pH	$k_{cat} \times 10^3$ (s^{-1})	$S_{0.5}$ (mM)	$k_{cat}/S_{0.5} \times 10^3$ (mM^{-1} s^{-1})	n_H	K_i (mM)	$k_{cat}/A \times 10^3$ (mM^{-2} s^{-1})	$k_{cat}/B \times 10^3$ (mM^{-1} s^{-1})
5.0	15.1 ± 4.2	3.88 ± 0.24	3.8 ± 1.1	1.36 ± 0.20	176 ± 44	6.5 ± 1.5	
5.4	36.3 ± 11.4	4.58 ± 1.05	7.9 ± 5.4	1.20 ± 0.23	61 ± 27	9.1 ± 3.5	3.6 ± 1.4
5.7	61.3 ± 8.5	4.88 ± 1.32	12.6 ± 5.1	1.07 ± 0.11	127 ± 63	50.0 ± 20.7	14.4 ± 2.7
6.0	71.8 ± 5.8	3.99 ± 0.59	18.0 ± 4.1	1.17 ± 0.07	86 ± 21	62.5 ± 17.1	17.9 ± 2.3
6.3	73.6 ± 3.0	3.72 ± 0.23	19.8 ± 2.0	1.68 ± 0.09	1090 ± 1082	9.9 ± 0.95	20.4 ± 7.7
6.6	75.9 ± 6.2	4.32 ± 0.51	17.6 ± 3.5	1.72 ± 0.17	300 ± 179	7.4 ± 1.4	30.0 ± 13.0
6.9	102 ± 13.1	6.76 ± 1.59	15.1 ± 5.5	1.12 ± 0.09	152 ± 68		12.6 ± 2.6
7.2	85.9 ± 8.7	9.85 ± 1.87	8.7 ± 2.5	1.04 ± 0.05	248 ± 113		9.1 ± 1.2
7.5	59.4 ± 15.5	10.71 ± 3.32	5.5 ± 3.1	1.63 ± 0.23	84 ± 54	3.4 ± 0.45	8.1 ± 2.8

Table 4: Steady-State Kinetic Parameters for the H115F Variant of YPDC

pH	$k_{cat} \times 10^3$ (s^{-1})	$S_{0.5}$ (mM)	$k_{cat}/S_{0.5} \times 10^3$ (mM^{-1} s^{-1})	n_H	K_i (mM)	$k_{cat}/A \times 10^3$ (mM^{-2} s^{-1})	$k_{cat}/B \times 10^3$ (mM^{-1} s^{-1})
5.0	6.8 ± 0.3	1.32 ± 0.15	5.1 ± 0.8	1.06 ± 0.08	72 ± 11		4.9 ± 0.9
5.4	14.7 ± 0.6	1.67 ± 0.13	8.7 ± 1.0	1.33 ± 0.10	239 ± 67	21.2 ± 10.5	10.1 ± 3.2
5.7	23.0 ± 0.7	2.32 ± 0.13	9.9 ± 0.8	1.42 ± 0.07	242 ± 42	13.2 ± 3.4	12.4 ± 2.9
6.0	32.5 ± 0.4	2.61 ± 0.07	12.4 ± 0.5	1.49 ± 0.04	905 ± 210	11.8 ± 1.5	17.5 ± 2.6
6.3	38.7 ± 0.1	3.14 ± 0.03	12.3 ± 0.1	1.60 ± 0.02	74690 ± 68400	7.1 ± 0.6	22.4 ± 3.6
6.6	47.6 ± 2.2	4.64 ± 0.34	10.3 ± 1.2	1.59 ± 0.09	230 ± 51	4.7 ± 0.2	14.6 ± 6.1
6.9	40.8 ± 0.3	5.35 ± 0.09	7.6 ± 0.2	1.59 ± 0.03	377200 ± 115400	2.7 ± 0.2	14.0 ± 3.2
7.2	38.4 ± 2.3	8.24 ± 0.73	4.6 ± 0.7	1.53 ± 0.07	205 ± 48	1.5 ± 0.4	5.5 ± 2.6
7.5	33.3 ± 1.2	10.94 ± 0.52	3.0 ± 0.2	1.73 ± 0.05	547 ± 160	0.45 ± 0.07	5.2 ± 2.1

Table 5: Steady-State Kinetic Parameters for the E477Q Variant of YPDC

pH	$k_{cat} \times 10^3$ (s^{-1})	$S_{0.5}$ (mM)	$k_{cat}/S_{0.5} \times 10^3$ (mM^{-1} s^{-1})	n_H	K_i (mM)
5.0	11.4 ± 0.7	0.93 ± 0.099	12.1 ± 1.4	1.31 ± 0.13	105.7 ± 33.72
5.4	51.3 ± 2.6	2.64 ± 0.32	19.4 ± 2.5	1.11 ± 0.17	50.78 ± 19.79
5.7	70.7 ± 2.2	2.88 ± 0.31	24.7 ± 2.7	1.31 ± 0.13	107.3 ± 34.58
6.0	85.6 ± 3.9	3.02 ± 0.22	28.6 ± 2.4	1.49 ± 0.11	213.7 ± 74.53
6.3	93.1 ± 2.5	3.22 ± 0.10	29.0 ± 1.2	1.75 ± 0.10	325.2 ± 111.2
6.6	93.3 ± 2.2	3.37 ± 0.11	28.3 ± 1.1	2.16 ± 0.09	1699.8 ± 1054.1
6.9	95.4 ± 3.0	4.66 ± 0.19	20.4 ± 1.1	2.23 ± 0.13	2007.1 ± 1069.4
7.2	87.7 ± 0.4	6.28 ± 0.067	13.8 ± 0.16	2.60 ± 0.06	76500.2 ± 47260.6
7.5	85.0 ± 0.8	10.76 ± 0.18	7.9 ± 0.15	2.63 ± 0.09	53810.5 ± 34280.1

Table 6: pK_a Apparent Data for WT YPDC and Variant Enzymes[a]

	from k_{cat}		pH-independent	from $k_{cat}/S_{0.5}$		$k_{cat}/S_{0.5}^n$		k_{cat}/A
	pK_{a1}	pK_{a2}	k_{cat} (s^{-1})	pK_{a1}	pK_{a2}	pK_{a1}	pK_{a2}	pK_{a2}
WT	5.34 ± 0.063	7.88 ± 0.1	45.45 ± 1.79	5.76 ± 0.11	6.23 ± 0.096			6.45 ± 0.43 (1.64 ± 0.12)
D28A	6.10 ± 0.079		0.13 ± 0.012	5.15 ± 0.087	7.19 ± 0.072		6.55 ± 0.11	
E477Q	5.39 ± 0.35 (2.3 ± 0.14)		0.091 ± 0.002	5.39 ± 0.042	6.92 ± 0.036		6.59 ± 0.48 (2.14 ± 0.13)	
H114F	5.74 ± 0.10	7.64 ± 0.21	0.11 ± 0.014	5.90 ± 0.043	6.78 ± 0.046			
H115F	5.84 ± 0.035	7.66 ± 0.08	0.055 ± 0.0026	5.36 ± 0.052	6.83 ± 0.042	5.19 ± 0.22	6.26 ± 0.13	

[a] pK_{a1} and pK_{a2} refer to the constants determined on the ascending (acid limb) and descending (alkaline limb) sides of the bell-shaped curves in Figures 3−7. pK_as from k_{cat} and $k_{cat}/S_{0.5}$ are weight-fitted according to the standard deviation of each data point. Values are only reported for experiments yielding reproducible values. Where there are no values listed, either there was no significant change from the plateau (the alkaline side of the k_{cat}−pH curves), or the data were insufficient to provide statistically significant numbers. In most cases reported, single proton ionizations fitted the data shown. For cases where the slopes were significantly greater than unity, an averaged value is shown with the slope in parentheses under the number quoted.

reported for the spontaneous hydration of carbon dioxide. The observation that WT YPDC releases CO_2 rather than HCO_3^- confirms early results of Krebs and Roughton (*38*), and rules out participation of the D28 and E477 side chains in hydration of carbon dioxide.

Rate of H/D Exchange at the C2 ThDP Position. The rate of H/D exchange at the thiazolium C2 position is an indicator of the rate of the first key step in any ThDP-dependent reaction. Such studies have been carried out on several ThDP-dependent enzymes using the method first reported from the Halle laboratories (*11*). Importantly for this study, the rate constant has been measured at 5.5 °C for some of the variants studied here. These rate constants are (s^{-1}) in the absence and in the presence of an 83 mM aliquot of the substrate surrogate pyruvamide [latter values in parentheses; pyruvamide is a molecule that cannot be decarboxylated yet activates the enzyme (*30*)]: D28A, 0.9 ± 0.1 (19 ± 2); E477Q, 0.9 ± 0.1 (19 ± 2); wild-type YPDC, 1.0 ± 0.1 (600). The rate constant in the absence of pyruvamide is most relevant to this discussion, showing that the k_{cat}s for these enzymes are very much smaller than these exchange rate constants; hence, neither

D28 nor E477 could be implicated in catalyzing the dissociation of C2H. Also, while the rate of C2H ionization could be rate-limiting on the unactivated enzyme, it is not rate-limiting on the activated forms of the enzyme variants examined here.

CONCLUSIONS

It is evident that the four residues D28, H114, H115, and E477, found at the active center, all have dramatic effects on rate-limiting steps, both from the binding of the first substrate through decarboxylation (*V/K* effects) and from decarboxylation through product release (effects on *V*), as also found with ZmPDC, with which YPDC shares a similar active center architecture (*25*, *26*). The decrease in the rate constants unequivocally shows the importance of the four residues in catalysis, more than likely in at least two steps each. As will be seen in the accompanying papers (*41*, *42*), many of the other features are not shared by YPDC and ZmPDC, signaling once more how important the substrate activation by YPDC is to virtually all aspects of its reactivity. We can only speculate why the various rate−pH profiles are little changed with the variants compared to WT YPDC, notwithstanding the large decrease in rate constants. Two likely scenarios are the following: (1) compensation of charges within the active center, i.e., when one partner in an ion-pair is mutated, the other partner's p*K* is significantly perturbed, so as to keep the overall charge in the active center unchanged; or (2) if the Asp(Glu) or His were neutral to start with, substitution with a side chain that is always neutral (such as Q,A,F in this study) will have no perceptible effects on the pH profiles. It will be shown in the next paper of this series (*41*) that the carboligase side reaction provides some additional insight to the charge distribution for residue D28, consistent with the second scenario.

It is instructive to compare our results with those on ZmPDC. Given the similarities in the active centers (H114... H113...D27...E473 in ZmPDC and H114...H115...D28...E477 in YPDC), one may have expected more similar behavior. Although the variants at the corresponding sites exhibit similar orders of magnitude reductions in specific activities, substitutions at H113 and H114 in ZmPDC exhibit different behavior from the corresponding H115 and H114 in YPDC. While the H114F and H115F YPDC variants could be purified, the H113Q ZmPDC variant was reported inactive. Perhaps even more significant is the difference in the $k_{cat}/S_{0.5}$−pH profiles: these are bell-shaped for WT YPDC and all of the variants studied here, whereas *V/K* shows a steady increase with increasing pH (to 8.5) for the ZmPDC (*26*). At present, we have no explanation for these differences.

As a working hypothesis for ThDP-dependent pyruvate decarboxylating enzymes, we suggest that, through the decarboxylation step, the constellation of residues His114...His115... D28 in YPDC (perhaps along with some specifically bound water molecules between) has a function akin to the oftencited 'oxyanion hole' in the serine proteases, i.e., to partially neutralize the incoming negative charge on the substrate, and on C2α-lactyl-ThDP, as it is being formed. As will be seen in the second paper in the series (*41*), D28 and E477 must also have a major role in some event(s) starting with the decarboxylation step and culminating in product release.

What is rather clear from both the steady-state kinetics and the C2 H/D exchange data is that neither D28 nor E477 (nor H114 and H115, based on more limited data) participates in the important first step (denoted by k_1) in Scheme 1: dissociation of the weak carbon acid to the corresponding conjugate base. These results further suggest that this important role be carried out by the only remaining catalytic site conjugate base, i.e., the iminopyrimidine ring of ThDP as an intramolecular base catalyst in YPDC, and, by extension, in all ThDP-dependent reactions. As was suggested from the Rutgers laboratory recently, this unusual reactivity of the coenzyme is likely to be related to the strong hydrophobic environment at the active center, that would be expected to modulate the relevant pK_a's, thereby stabilizing the key zwitterionic intermediates (*40*).

REFERENCES

1. Krampitz, L. O. (1969) *Annu. Rev. Biochem. 38*, 213−240.
2. Sable, H. Z., and Gubler, C. J. (1982) *Ann. N.Y. Acad. Sci. 378*, 7−122.
3. Kluger, R. (1987) *Chem. Rev. 87*, 863−876.
4. Schellenberger, A., and Schowen, R. L., Eds. (1988) *Thiamin Pyrophosphate Biochemistry*, Vol. 1 and 2, CRC Press, Boca Raton, FL.
5. Bisswanger, H., and Ullrich, J., Eds. (1991) *Biochemistry and Physiology of Thiamin Diphosphate Enzymes*, pp 1−453, VCH Publishers, Weinheim, Germany.
6. Bisswanger, H., and Schellenberger, A., Eds. (1996) *Biochemistry and Physiology of Thiamin Diphosphate Enzymes*, pp 1−599, A.u.C. Intemann, Wissenschaftlicher Verlag, Prien, Germany.
7. Breslow, R. (1958) *J. Am. Chem. Soc. 80*, 3719−3726.
8. Dyda, F., Furey, W., Swaminathan, S., Sax, M., Farrenkopf, B., and Jordan, F. (1993) *Biochemistry 32*, 6165−6170.
9. Arjunan, D., Umland, T., Dyda, F., Swaminathan, S., Furey, W., Sax, M., Farrenkopf, B., Gao, Y., Zhang, D., and Jordan, F. (1996) *J. Mol. Biol. 256*, 590−600.
10. Killenberg-Jabs, M., König, S., Eberhardt, I., Hohmann, S., and Hübner, G. (1997) *Biochemistry 36*, 1900−1905.
11. Kern, D., Kern, G., Neef, H., Tittmann, K., Killenberg-Jabs, M., Wikner, C., Schneider, G., and Hübner, G. (1997) *Science 275*, 67−70.
12. Gao, Y. (2000) Ph.D. Dissertation, Rutgers University, Newark, NJ.
13. Guo, F., Zhang, D., Kahyaoglu, A., Farid, R. S., and Jordan, F. (1998) *Biochemistry 37*, 13379−13391.
14. Zeng, X., Farrenkopf, B., Hohmann, S., Dyda, F., Furey, W., and Jordan, F. (1993) *Biochemistry 32*, 2704−2709.
15. Baburina, I., Gao, Y., Hu, Z., Jordan, F., Hohmann, S., and Furey, W. (1994) *Biochemistry 33*, 5630−5635.
16. Baburina, I., Moore, D. J., Volkov, A., Kahyaoglu, A., Jordan, F., and Mendselsohn, R. (1996) *Biochemistry 35*, 10249−10255.
17. Baburina, I., Li, H., Bennion, B., Furey, W., and Jordan, F. (1998) *Biochemistry 37*, 1235−1244.
18. Baburina, I., Dikdan, G., Guo, F., Tous, G. I., Root, B., and Jordan, F. (1998) *Biochemistry 37*, 1245−1255.
19. Jordan, F., Nemeria, N., Guo, F., Baburina, I., Gao, Y., Kahyaoglu, A., Li, H., Wang, J., Yi, J., Guest, J., and Furey, W. (1998) *Biochim. Biophys. Acta 1385*, 287−306.
20. Li, H., Furey, W., and Jordan, F. (1999) *Biochemistry 38*, 9992−10003.
21. Li, H., and Jordan, F. (1999) *Biochemistry 38*, 10004−10012.
22. Wang, J., Golbik, R., Seliger, B., Spinka, M., Tittmann, K., Hübner, G., and Jordan, F. (2001) *Biochemistry 40*, 1755−1763.
23. Alvarez, F. J., Ermer, J., Hübner, G., Schellenberger, A., and Schowen, R. L. (1995) *J. Am. Chem. Soc. 117*, 1678−1683.
24. Washabaugh, M. W., and Jencks, W. P. (1988) *Biochemistry 27*, 5044−5053.

25. Chang, A. K., Nixon, P. F., and Duggleby, R. G. (1999) *Biochem. J. 339*, 255−260.
26. Schenk, G., Leeper, F. J., England, R., Nixon, P. F., and Duggleby, R. G. (1997) *Eur. J. Biochem. 248*, 73−81.
27. Lobell, M., and Crout, D. H. G. (1996) *J. Am. Chem. Soc. 118*, 1867−1873.
28. Sarkar, G., and Sommer, S. S. (1990) *BioTechniques 8*, 404−407.
29. Clontech Laboratories, Palo Alto, CA, manuals for Talon chromatography.
30. Hübner, G., Weidhase, R., and Schellenberger, A. (1978) *Eur. J. Biochem. 92*, 175−181.
31. Bradford, M. M. (1976) *Anal. Biochem. 72*, 248−254.
32. Holzer, H., Schultz, G., Villar-Palasi, C., and Jutgen-Sell, J. (1956) *Biochem. Z. 327*, 331−344.
33. Ellis, K. J., and Morrison, J. F. (1982) *Methods Enzymol. 87*, 405−427.
34. Yan, R.-T., Zhu, C.-X., and Chen, J.-S. (1987) *Anal. Biochem. 164*, 362−366.
35. Henehan, G. T. M., Chang, S. H., and Oppenheimer, N. O. (1995) *Biochemistry 34*, 12294−12301.
36. Novagen, Madison, WI.
37. Farrenkopf, B., and Jordan, F. (1992) *Protein Expression Purif. 3*, 101−107.
38. Krebs, H. A., and Roughton, F. J. W. (1948) *Biochem. J. 43*, 550.
39. Dobritzsch, D., Konig, S., Schneider, G., and Lu, G. (1998) *J. Biol. Chem. 273*, 20196−20204.
40. Jordan, F., Li, H., and Brown, A. (1999) *Biochemistry 38*, 6369−6373.
41. Sergienko, E. A., and Jordan, F. (2001) *Biochemistry 40*, 7369−7381.
42. Sergienko, E. A., and Jordan, F. (2001) *Biochemistry 40*, 7382−7403.

BI002855U